Antifouling membranes prepared by electrospinning PLA containing biocidal nanoparticles

Please, cite as follows:

Aravind Dasari, Jennifer Quirós, Berta Herrero, Karina Boltes, Eloy García-Calvo, Roberto Rosal. Antifouling membranes prepared by electrospinning polylactic acid containing biocidal nanoparticles. Journal of Membrane Science, 405–406, 134-140, 2012. https://doi.org/10.1016/j.memsci.2012.02.060.

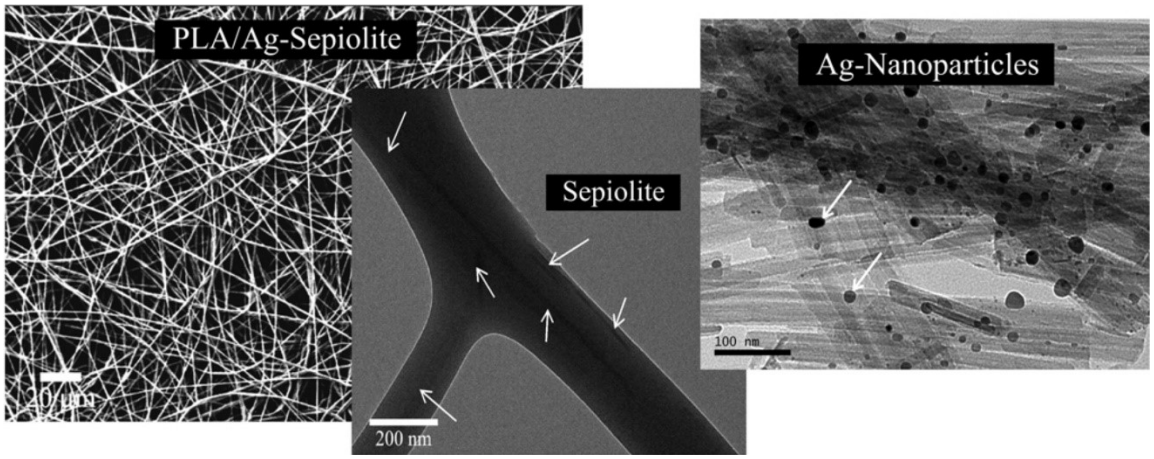

https://www.sciencedirect.com/science/article/pii/S0376738812001767

Antifouling membranes prepared by electrospinning PLA containing biocidal nanoparticles

Aravind Dasaria[1,a], Jennifer Quirós[2], Berta Herrero[1], Karina Boltes[2], Eloy García-Calvo[3], Roberto Rosal,[2,3,*]

[1] Madrid Institute for Advanced Studies of Materials (IMDEA Materials Institute), Profesor Aranguren s/n, E-28040, Madrid, Spain

[2] Department of Analytical Chemistry, Physical Chemistry and Chemical Engineering, University of Alcalá, Alcalá de Henares, E-28871 Madrid, Spain

[3] Madrid Institute for Advanced Studies of Water (IMDEA Water Institute), Parque Científico Tecnológico, E-28805, Alcalá de Henares, Madrid, Spain

[*] Corresponding author: roberto.rosal@uah.es

Abstract

We prepared non-woven electrospun polylactic acid (PLA) membranes containing functionalized sepiolite fibrillar particles (5 wt%). Biocidal activity was achieved by functionalizing sepiolite fibers with Ag (26 wt%) and Cu (26 wt%), which were embedded in the fiber surface. Sepiolite particles were negatively charged in all cases, with zeta potential in the range of −15 to −37 mV, increasing their negative charge with pH. The membranes were biofouled in a crossflow filtration device using model biofoulants, cultures of Saccharomyces cerevisiae (pH 4.5) and *Pseudomonas putida* (pH 7.5), which were pumped across the membrane for 24/48 h. The assessment of active biomass was performed by measuring the concentration of adenosine-5′-triphosphate (ATP) in used membranes. The results showed a significant decrease in the amount of surface ATP for PLA loaded with Ag and Cu functionalized sepiolite. The effect was particularly intense for Ag-sepiolite in contact with Saccharomyces cerevisiae, where the reduction amounted to 85% compared to neat PLA (control). This was attributed to the differences in ion availability as a function of pH and to the presence of chloride ions in solution. Pristine sepiolite (without functionalization) did not show any noticeable effect.

***Keywords**:* Electrospinning; Polylactic acid; Membranes; Biocidal nanoparticles; Anti-biofouling

1. Introduction

Membrane technologies have been used to meet the increasingly stringent regulatory requirements for drinking water production as well as for wastewater treatment, particularly for cases of restrictive discharge limits such as those for nitrogen and phosphorus. Microfiltration and ultrafiltration are good examples of methods which achieve a high level of pathogen removal without requiring chemical pretreatment or with a reduced disinfectant dosage [1]. Membrane Biological Reactors (MBR) have been replacing conventional treatment plants in a cost-effective process which combines clarification, aeration, and filtration in a single unit. They show a high capacity to remove dissolved organic matter, suspended solids, and heavy metals providing a high quality effluent suitable for discharge or reuse [2], [3]. Recently, nutrients and individual micropollutants of anthropogenic origin have emerged as a cause of increasing concern in wastewater treatment because the effluent of treatment plants is the entry point to the natural environment for many compounds such as pharmaceuticals and personal care products the long term effects of which are essentially unknown [4]. Concerning non-polar compounds, MBR have shown greater removal performances as a result of increased adsorption due to the relatively high solid retention times intrinsically associated with this process [5].

Despite the advantages of membrane processes, their application is hindered by the difficulty of controlling membrane fouling. Three main mechanisms for the fouling of porous membranes have generally been noted: (1) pore constriction due to the adsorption of chemical species within the membrane pores, (2) pore blocking at the membrane surface, and (3) cake formation by the rejected species [6]. Fouling is caused by the accumulation of organic and inorganic substances, including particles as well as biofilm formation due to the deposition or growth of microorganisms. The organic compounds involved in fouling may come from natural organic matter, but in the case of wastewater treatment they are mostly formed by a class of macromolecular compounds known as extracellular polymeric substances (EPS). EPS are produced by microorganisms and mainly consist of polysaccharides and to a lesser extent,

[a] Current address: School of Materials Science and Engineering (Blk N4.1), Nanyang Technological University, 50 Nanyang Avenue, 639798 Singapore.

https://doi.org/10.1016/j.memsci.2012.02.060

nucleic acids, and proteins [7]. Unlike physical or chemical fouling, biofouling often causes irreversible damage to the membranes. Biofouling is a major challenge in membrane water treatment systems as it leads to the need for higher operating pressures and frequent backwashing or chemical cleanings. Backwashing is the usual strategy employed to control biofouling, but flow recovery is never complete because certain compounds become irreversibly attached to the membrane [8]. Another strategy to prevent membrane biofouling is pretreatment of the feed stream with conventional biocidal chemicals such as chlorine. This approach has many drawbacks, including the damage suffered by membranes, particularly those based on polyamide the possibility of formation of harmful oxidation by-products [9]. It should also be noted that while a biocide may kill the biofilm organisms, it will not usually remove the bio-fouling layer [10].

Generally, the surface properties of membranes determine their performance under fouling or biofouling conditions. It has been observed that hydrophilic membrane surfaces are less prone to the microbial adhesion triggering biofouling [10]. Moreover, as most commercial polymeric membranes are hydrophobic, considerable interest has been shown in developing new membranes or modifying existing ones to increase their hydrophilicity [11], [12]. Surface charge determines microbial adhesion because cell membranes possess large negatively charged domains, which are repelled by surfaces bearing negative charges such as those obtained by graft polymerization of acrylic acid [13]. Nevertheless, it has also been reported that positively charged surfaces result in strong electrostatic attractive forces that hinder microbial replication [14]. Another approach consists of incorporating anti-biofouling substances to prevent microbial growth. For example, the incorporation of silver ions in hydrophilic membranes enhances their charge-driven anti-adhesive properties and provides a specific anti-microbial function. This acts as a safeguard in case some bacteria become attached to membrane surface [15].

Therefore, in the current study, PLA and sepiolite were strategically chosen for the preparation of reinforced porous membranes. PLA shows higher natural hydrophilicity than conventional thermoplastic polymers. This is due to the access of water molecules to polar oxygen linkages in PLA, which can help in improving fluxes and reducing the biofouling tendency of the membrane [16]. Sepiolite particles have an average length of 1–2 μm, width ~10 nm, and the dimensions of open channels (along the axis of a particle) ~3.6 Å × 10.6 Å. The arrangement of these particles results in loosely packed and porous aggregates with an extensive capillary network. In addition, the high density of silanol groups (-SiOH) on the surface enhances its hydrophilicity. These remarkable characteristics of sepiolite have made it an ideal choice for many technological applications such as photocatalysis, heavy metal adsorption, metallic nanoparticle support with biocide or plasmonic properties, and vaccine support. To address the problems associated with biofouling, Ag and Cu functionalized sepiolite were utilized. As model biofoulants, we used suspensions of the yeast *Saccharomyces cerevisiae* and the bacterium *Pseudomonas putida*. The extent of fouling was assessed by measuring permeate flow and by extracting the active biomass deposited on the membrane.

2. Materials and methods

2.1 Materials

Transparent PLA (trade name: 'PLA Polymer 2002D') was purchased in the form of pellets from NatureWorks LLC, UK with a melt index of 5–7 g/10 min (at 210 °C/2.16 kg). This grade is derived from annually renewable resources and has a D-content of 4% (96% L-lactide content). It has a molecular weight of ~121,400 g/mol and a melting temperature of 160 °C. Refined, unmodified and functionalized sepiolite particles were obtained from Tolsa S.A, Spain. Ag (26 wt%) and Cu (26 wt%) functionalized sepiolite were prepared by means of a reduction process followed by a dehydration of the matrix. The structure of sepiolite consists of an arrangement of blocks separated by parallel channels formed by two layers of tetrahedral SiO_2 enclosing a layer of octahedral MgO. A lixiviation step of Mg^{2+} is required prior to the introduction of other metallic cations due to the relatively narrow size of open channels [17]. The procedure of lixiviation by acid treatment and the maximum amount of Mg^{2+} which can be removed from sepiolite without modifying its crystalline structure have been discussed in detail elsewhere [18]. The host particles were conditioned to support dispersed metallic nanoparticles using metal alkoxides as starting reagents in which the organic moieties facilitate their diffusion. The incorporation of small amounts of water provokes a controlled hydrolysis and polycondensation of the alkoxide, which is detected by a sudden heterocoagulation of the gel (typically at temperatures below 80 °C). After the incorporation of silver or copper, a thermal treatment allows generating the corresponding nanoparticles which are metallic if the treatment takes place under reducing atmosphere. As a consequence of thermal treatment, the structure loses water and transforms into an anhydrous sepiolite. The advantage of this process is that the nanoparticles are embedded in the silicate particles, rather than being loosely held. In our case nanoparticle size distribution was relatively broad, ranging from 3 to 50 nm [19].

Dichloromethane (DCM, 99.5%) and ethanol (EtOH, 96%) were analytical grade and obtained from Sigma–Aldrich and used as received. Culture media components YNB (yeast nitrogen base) and CSM-URA

https://doi.org/10.1016/j.memsci.2012.02.060

(complete supplement medium without uracil) were purchased from MP Biomedicals. The rest of the culture media components were analytical grade reagents purchased from Panreac, Scharlau, Fluka of Sigma–Aldrich.

2.2. Electrospinning

A NANON-01A electrospinning unit (Mechanics Electronic Computer Corporation, MECC Co. Ltd., Japan) was used for this purpose. To produce porous fibrous membranes which would provide easy access to functionalized nanoparticles, a dual solvent approach was employed. 7 wt% of PLA solution was prepared by dissolving the required amount of PLA pellets in DCM followed by constant magnetic stirring for 24 h. 0.35 g of sepiolite or functionalized sepiolite particles were dispersed in 5 g distilled water using an ultrasonic bath for 45 min. Afterwards, 5 g ethanol (50% w/w in water) was added to the solution and sonicated in an iced water bath for another 45 min to avoid solvent evaporation. Subsequently, 1 g of this solution was mixed with 9 g of PLA solution (to maintain the final weight concentration of PLA/sepiolite or PLA/functionalized sepiolite fibers at 95/5). This was again sonicated in an iced water bath for 20 min followed by another 15 min of magnetic stirring before electrospinning using the following parameters: voltage ~21 kV; feed rate ~0.9 ml/h; distance between the tip of the needle and drum collector ~15 cm; and drum rotation speed ~300 rpm.

2.3. Analytical methods

The morphology of porous nanofibers after sputter coating was examined using a scanning electron microscope (SEM) from Carl Zeiss (EVO MA15) at an accelerating voltage of 5 kV and probe intensity of 50 pA. Nanoparticles and selected fibrous samples were also observed at an accelerating voltage of 100 kV using a JEOL JEM-1010 transmission electron microscope (TEM), which is capable of obtaining digital images. Nitrogen adsorption isotherms were measured at 77 K using a Beckman-Coulter SA3100 system on samples after outgassing overnight at 200 °C. Particle counting was performed using a Z2 Coulter Counter Analyzer in line with International Standard ISO 13319:2000. Zeta potential was measured via electrophoretic light scattering combined with phase analysis light scattering using the same instrument. The measurements were conducted at 25 °C using 10 mM in KCl as dispersing medium. The extent of biofouling was assessed using a Molecular Probes ATP Determination Kit (A22066), which offers a bioluminescence assay for quantitative determination of ATP with recombinant firefly luciferase and D-luciferin. ATP provides a direct measure of the amount of active biomass. The assay is based on the ATP requirement of luciferase to produce light (emission maximum ~560 nm), which was recorded using a Fluoroskan Ascent FL fluorometer/luminometer.

2.4. Preparation of microbial biofoulants and experimental procedure

The model biofoulants used in this study were *Saccharomyces cerevisiae* and *Pseudomonas putida*, preserved at −80 °C to be later reactivated in small volume flasks using optical density (OD) as endpoint. *S. cerevisiae* was grown in rotary shakers at 30 °C, 200 rpm and pH 4.5 using the following culture medium: CSM-URA: 0.78 g/L; YNB: 6.7 g/L; sucrose: 20 g/L. *P. putida* was reactivated at 30 °C in a Luria–Bertani saline medium containing 15 μg/mL tetracycline. After optical density reached the prescribed value (OD 0.5), *S. cerevisiae* was transferred to a 1 L flask in the membrane biofouling device using the same medium and *P. putida* (OD 1.0) to a basal salt medium (BSM) containing 20 g/L L-glutamic acid as source of carbon and 440 mg/L of $MgSO_4 \cdot 7\ H_2O$ as source of sulphur with pH adjusted to 7.5. An aliquot of grown cultures was diluted in culture medium and finally transferred to a 1 L thermostated beaker as described below.

The experimental device for membrane biofouling consisted in a stainless steel cross-flow microfiltration device for 90 mm circular membranes acquired to Millipore. The reason for using a cross-flow configuration was to keep a certain flow across the membrane to avoid excessive accumulation of biomass, which could eventually block biocidal sites. Pore blocking would also require an increase in transmembrane pressure, which was not desired as membranes were not strong enough to resist an overpressure over the design value. The membrane was supported on a PTFE holder which allowed the suspension of microorganisms in their culture media to be circulated across the membrane. Both filtered liquid and rejected culture were recovered in a 1 L beaker kept at 30 °C by means of a Polystar cc2 thermostat, agitated using a magnetic rod and recirculated to the filtration unit using a Stepdos diaphragm-metering pump with a flow rate of 8.0 mL/min. The beaker was aerated, but culturing *P. putida*, a 100 L/h flow of 0.45 μm filtered air was ensured throughout the run. The device allowed a transmembrane pressure drop of 50 kPa under normal operating conditions. Sterile teflon filters (0.45 μm) were used for filtering the bubbled air and for venting. All membranes were kept in contact with circulating cultures of *S. cerevisiae* (48 h) and *P. putida* (24 h) before opening the unit and removing membrane for analysis. The reason for choosing contact time of 24/48 h was to ensure that both organisms were in logarithmic growing phase into the beaker. In such conditions, cells were in their best physiological state and replication occurred at high rate. In separate runs, we proved that during the first 24 h of culture, cells of *P. putida* remain in exponential growing phase, clearly marked by the increment of dry-weight of biomass and a high oxygen demand. After roughly 30 h, *P. putida* reached stationary phase as evidenced

by a sharp reduction of oxygen demand. After about 24 h, *S. cerevisiae*, started the diauxic growth phase in which it uses ethanol as carbon source and reached the stationary phase at about 50 h. An increment of culture time over the values used in this work would eventually result in nutrient limitation and loss of their adhesion capabilities to form biofilms.

Biofouled membranes were washed carefully with ultrapure water and cut into four equal fragments for ATP determination. Samples of the culture media were also analysed for their ATP content using the same analytical probe in samples obtained from the liquid remaining in the beaker after stopping flow and draining all lines to it. The permeability of used membranes was assessed in a 47 mm dead-end filtration setup loaded with a total volume of 100 mL of distilled water with a transmembrane pressure drop of −30 kPa. For these runs, the membrane area was 45.5 cm^2.The time required to completely drain the load of water was recorded four times with two independent fragments of biofouled membranes and compared with raw, unused membranes.

3. Results and discussion

The ζ-potential of sepiolite and metal loaded sepiolite particles is shown in Table 1. All particles were negatively charged, with values of ζ-potential below −30 mV at pH 7.5 and should not, therefore, present any electrostatic interaction with the negatively charged cell walls and membranes. However, it has also been shown that the possibility exists of cells interacting with negatively charged particles if they bind to cationic sites on the cell surface to form clusters favored by the repulsive interactions with negatively charged domains [20].

Table 1. ζ-potential of sepiolite and metal-loaded sepiolite.

Material	ζ-potential (pH 4.5, mV)	CI 95% (±)	ζ-potential (pH 7.5, mV)	CI 95% (±)
Sepiolite	−15.1	1.2	−30.0	0.8
Cu/Sep	−25.9	0.9	−36.7	1.1
Ag/Sep	−29.5	0.6	−37.3	0.4

SEM and TEM micrographs of sepiolite and functionalized sepiolite particles are shown in Fig. 1, Fig. 2, Fig. 3. As expected, small and monodispersed Ag and Cu nanoparticles were located on the sepiolite (silicate) surface (Fig. 1). It should be noted that the nanoparticles were not loosely held but were embedded in the silicate matrix due to the collapse of sepiolite structure over Ag and Cu nanoparticles via dehydration and reduction during the functionalization process [21]. This prevented their coalescence and further oxidation. The morphology of the fibers at different

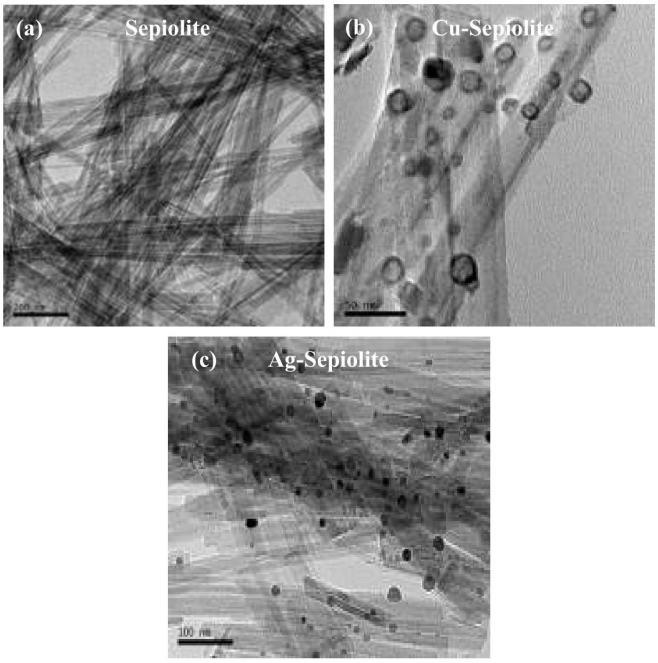

Figure 1. TEM micrographs of (a) sepiolite, (b) Cu/sepiolite, and (c) Ag/sepiolite particles.

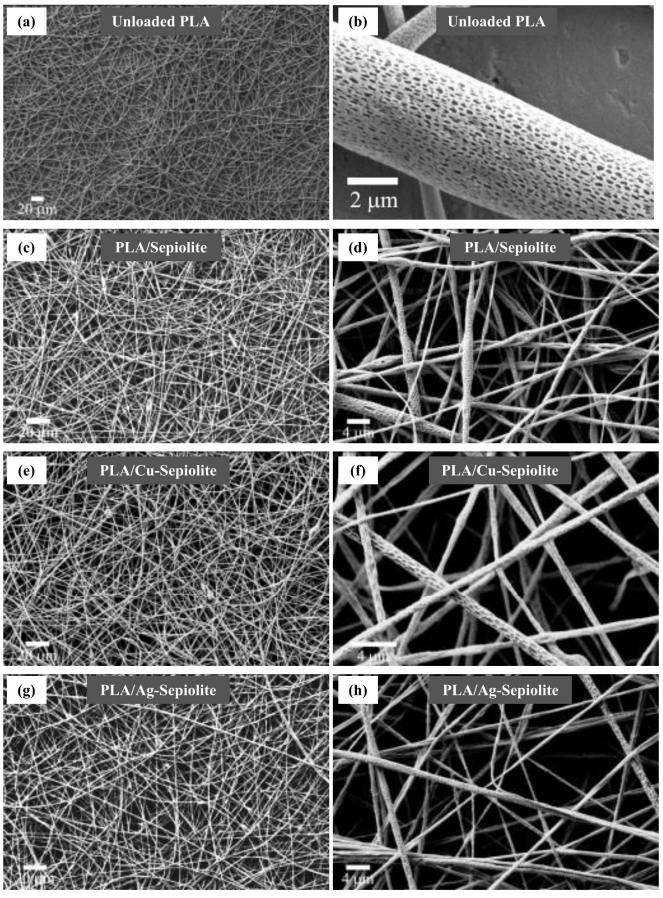

Figure 2. SEM micrographs of (a and b) unloaded neat PLA, (c and d) PLA/sepiolite, (e and f) PLA/Cu/Sep, and (g and h) PLA/Ag/Sep fibers.

magnifications after the incorporation of particles in PLA via electrospinning is shown in Fig. 2. Fibers were intentionally designed to be porous by choosing a combination of solvent systems with different vapor pressures for electrospinning. This was important to

https://doi.org/10.1016/j.memsci.2012.02.060

provide easy access for external medium to functionalized biocidal nanoparticles. In all cases (unreinforced and reinforced), fibers were mostly bead-less, despite the inhomogeneity in fibre diameters. This is a disadvantage with the mixed solvent approach adopted, as it depends on the location of high or low vapor pressure solvent. In fact, this also results in the lack of control over the pore size. However, as expected, pores were slightly elongated along the fibre direction due to the electrospinning process. Fig. 3 shows a representative TEM micrograph of PLA/sepiolite fibers, which indicates good defibrillation and distribution of sepiolite particles in the fibers. Apart from ultrasonication and magnetic stirring, using PLA as matrix, strong interaction (and therefore good dispersion) with even unmodified sepiolite was expected, originating from the hydrogen bonding between the polymer C=O groups and the sepiolite hydroxyl groups. All membranes showed a rejection of >98% for particles exceeding 3 μm, determined by direct particle counting using Coulter Counter equipment and appropriate standards.

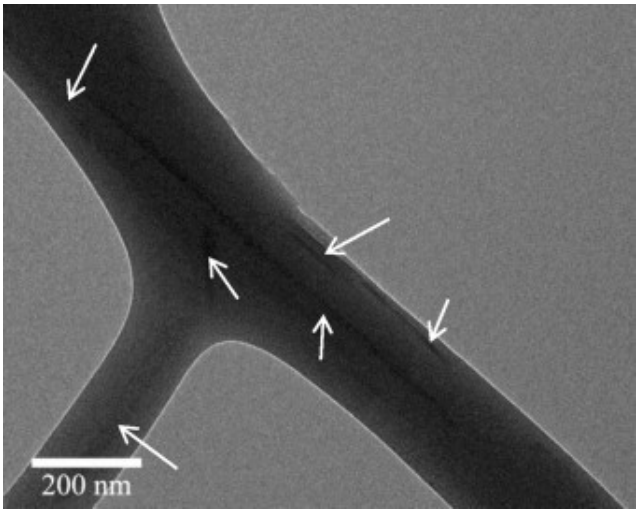

Figure 3. Representative TEM micrograph of PLA/sepiolite fibers showing the distribution of sepiolite particles (indicated with arrows).

The results obtained for ATP determination of biofouled membranes are shown in Fig. 4. ATP is a direct measure of active biomass and was expressed as ATP membrane/culture ratio (ATP_m/ATP_c). The reason for using relative values is the variability in absolute values from run to run due to the different final content of active biomass. ATP_m was measured as μmol cm^{-2} by computing the surface of membrane digested with the standard reaction solution prescribed by the manufacturer. The ratio (ATP_m/ATP_c) has, therefore, units of L cm^{-2} which correspond to the values indicated in Fig. 4. The average values for ATP membrane–ATP culture used to build-up the ratio shown in Fig. 4, are 0.35–0.66 (PLA), 0.46–084 (sepiolite), 0.25–0.65 (Cu/Sep), 0.22–0.63 (Ag/Sep) for *P. putida* and 0.61–0.29 (PLA), 0.60–0.28 (sepiolite), 0.42–0.33 (Cu/Sep), 0.17–0.52 (Ag/Sep) for *S. cerevisiae* expressed in μmol cm^{-2} and μmol L^{-1} respectively. The data clearly show the absence of biocidal effect of sepiolite loaded membranes, for which the biofouling ratios were very similar to those obtained by unloaded PLA mats. The data for membranes loaded with copper or silver functionalized sepiolite showed, however, significant differences, marked by asterisks. The effect was in both cases lower for *P. putida* (pH 7.5) than for *S. cerevisiae* (pH 4.5). Silver-sepiolite (Ag/Sep) yielded a 35% biofouling decrease in contact with *P. putida* and a remarkable 85% for *S. cerevisiae*. We observed a significant variation in ATP results for different fragments of the same biofouled membrane. Typical differences ranged from 0.3 to 0.7 expressed as coefficient of variation (CV), which was defined as the ratio of standard deviation to the mean. This was a consequence of the flow pattern, which induced preferential biofouling of certain parts of the membrane. The data shown in Fig. 4 were calculated with ATP from the sum of all fragments from the same membrane and are not affected by this heterogeneity.

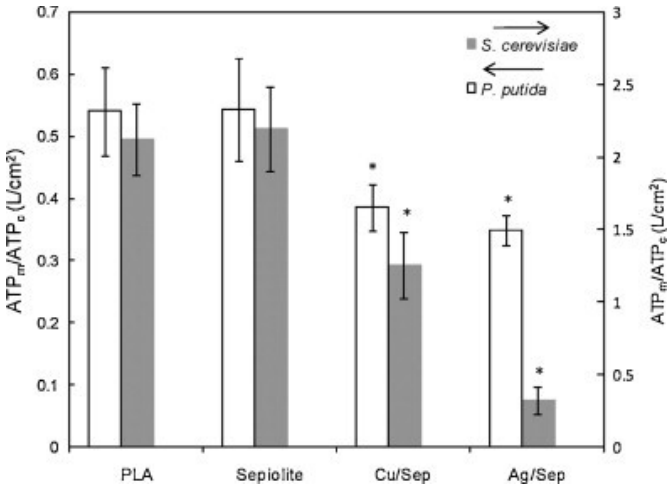

Figure 4. ATP ratio membrane/culture for raw and functionalized PLA membranes after biofouling with *S. cerevisiae* (48 h) and *P. putida* (24 h).

Considering the low probability of electrostatic interaction of microorganisms with the negatively charged sepiolite and metal-loaded sepiolite included in the membrane, the speciation of copper and silver as a function of pH was the sole factor determining the species reaching the solution and affecting microorganisms. It has been shown that the predominant form of copper at pH < 6.5 is Cu^{2+}, whereas at pH 7.5 aqueous $CuCO_3$ accounts for almost all dissolved copper [21]. In the presence of chloride, it has been shown that silver chloride is the predominant complex with a minor contribution of Ag^+ and $AgCl_2^-$. The speciation does not depend on pH or the content of silver ions, Ag^+, in solution which decreases with chloride concentration [21]. Based on these results, free Cu^{2+} ions could be detrimental for *S. cerevisiae*, which could partially explain the lower fouling obtained with respect to *P. putida*. The chloride content of BSM could

https://doi.org/10.1016/j.memsci.2012.02.060

also be responsible for silver complexation reducing silver bioavailability for *P. putida*. This would explain the results obtained for Ag/Sep membranes where *S. cerevisiae* induced a much lower biofouling.

The permeability of raw and biofouled membranes expressed as permeate flux, J_w, were calculated using the following equation:

$$J_w = \frac{(permeate\ volume)}{(area)(time)}$$

In order to take into account, the (slight) differences in permeability of clean membranes, the flux values of all the membranes were normalized to the flux value of the unmodified membrane as follows:

$$PI = \frac{J_f^{PLA}}{J_f^j}\frac{J_o^j}{J_o^{PLA}}$$

where "j" refers to sepiolite, Cu/Sep and Ag/Sep as appropriate and the subscripts "*o*" and "*f*" indicate the permeate flux for clean and used membranes, respectively. The permeability index (PI) was considered an experimental measure of reversible fouling. Used membranes were carefully washed with distilled water prior to permeability measurement. Pure water permeability values for unmodified and modified membranes are shown in Fig. 5 expressed as PI for sepiolite and metal-loaded sepiolite taking the permeability of PLA membrane as reference. Pure water permeability for clean membranes was 14.3, 11.2, 16.4 and 11.3 L m^{-2} h^{-1} kPa^{-1} for PLA, sepiolite, Cu/Sep and Ag/Sep respectively, whereas the permeability of fouled PLA membranes was 5.8 and 4.9 L m^{-2} h^{-1} kPa^{-1} (*P. putida* and *S. cerevisiae*). The permeability values displayed in Fig. 5 together with their 95% confidence intervals, indicated that the load of sepiolite did not have any significant effect on pure water permeability, with a decrease similar to that of PLA both for *S. cerevisiae* and for *P. putida*. For metal-loaded membranes and for both microorganisms, the reduction in permeability loss was statistically significant with respect to non-metal loaded sepiolite and unloaded PLA. For Cu/Sep and Ag/Sep loaded membranes, the water permeability after washing fouled membranes was roughly 50% of that encountered in PLA membranes. The relatively high dispersion of results as noted by the error bars in Fig. 5 was probably a consequence of the heterogeneity of 90 mm membranes, from which two independent pieces from each run were taken for permeability assessment.

It has been shown that nanocopper or nanosilver produce toxicity in aquatic organisms, whch is largely due to effects of particulates as opposed to release of dissolved ions. Griffitt et al. encountered different gene expression associated with the exposure of *Danio rerio* to nanometals and soluble metals, suggesting that each exposure produces toxicity by a different

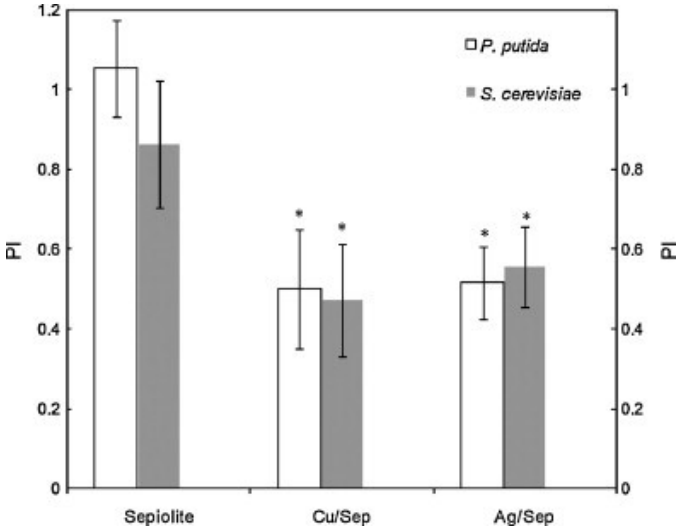

Figure 5. Permeability index (PI) determined from permeability measurements for raw and functionalized PLA membranes after biofouling with *S. cerevisiae* (48 h) and *P. putida* (24 h).

mechanism [22]. On the other hand, the cause of nanocopper toxicity has been associated with soluble Cu^{2+} in a number of studies [23]. Kasemets et al., however, attributed only 50% of the nanocopper oxide toxicity to *S. cerevisiae* to the soluble form of Cu^{2+}, the rest being associated with certain kinds of nanotoxicity [24]. Navarro et al. also showed that the toxicity of nanosilver particles was much higher than that of ionic Ag^+, so that dissolved silver could not fully explain the observed toxicity to the freshwater alga *Chlamydomonas reinhardtii* [25]. Our results cannot exclude any of both possibilities, but in our case the internalization of nanoparticles was not possible as they remained firmly attached to sepiolite fibers. The biological effect is most probably associated with the release of soluble metal ions into the water environment. Further research is required, however, to completely elucidate this question.

The environmental risk associated to the use of nanomaterials and the integrity of membrane biocidal function are additional issues associated to the use of nanoparticles in aqueous environments. Transmembrane pressure avoids the release of nanoparticles or the soluble forms of metals into the concentrate, for example the bioreactor in MBR processes. The major concern would be the passage of nanoparticles or soluble metals to treated wastewater and eventually to the environment. This problem is related to the release of silver or other metals from commercial products and have been dealt with elsewhere, being the subject of intense discussions [26]. Another question would be the stability of the biocidal layer. In MBR, the air bubbles emitted at the diffuser serve, besides providing aeration, to remove solids from the membrane surface and might eventually degrade the biocidal cover of the membrane and release nanoparticles to treated wastewater. This connects with a general problem, which is the discharge to wastewater

https://doi.org/10.1016/j.memsci.2012.02.060

of nanoparticles from consumer goods such as laundry detergents or water filters. Kaegi et al. [27] have recently shown that silver nanoparticles tend to sorb onto wastewater biosolids and to a large extent undergo chemical transformation into silver sulfide within wastewater treatment plants. The question of environmental fate of nanoparticles is outside the scope of this work but should be carefully addressed to before promoting the generalized use of biocidal nanotechnologies.

4. Conclusions

Electrospun polylactic acid (PLA) membranes loaded with sepiolite fibrillar particles functionalized with silver and copper were tested for anti-biofouling performance using the yeast *S. cerevisiae* and the bacterium *P. putida* as model microorganisms.

The concentration of ATP in membrane surface was used to assess active biomass content and showed a significant decrease for silver and copper functionalized sepiolite with respect to PLA. The highest effect was obtained for Ag-sepiolite in contact with *S. cerevisiae*, for which the ATP reduction reached to 85% compared to neat PLA. Sepiolite without functionalization did not show any significant effect.

The permeability of used Ag– and Cu–sepiolite membranes was also considerably enhanced with respect to PLA with flow approximately twice that measured for PLA and non-functionalized sepiolite under the same conditions.

The effect was attributed to the differences in ion availability as a function of pH and to the presence of chloride ions in solution. This is because nanoparticles are firmly attached to the matrix and cannot be internalized and the contact between microorganisms and nanosilver or nanocopper is hindered by the negative charge of sepiolite and functionalized sepiolite.

Acknowledgments

This work has been financed by Spain's Ministry of Education (CSD2006-00044 and CTM2005-03080/TECNO) and the Dirección General de Universidades e Investigación de la Comunidad de Madrid, Research network 0505/AMB-0395. AD acknowledges Tolsa, Madrid for the continued support, cooperation and provision of silicate particles.

References

[1] M.D. Kennedy, J. Kamanyi, S.G. Salinas-Rodríguez, N.H. Lee, J.C. Shippers, G. Amy. Water treatment by microfiltration and ultrafiltration. In: N.N. Li, A.G. Fane, W.S. Winston Ho, T. Matsuura (Eds.), Advanced Membrane Technology and Applications, John Wiley & Sons, NJ (2008), pp. 131-170.

[2] D.L. Russell. Practical Wastewater Treatment John Wiley & Sons, NJ (2006).

[3] P. Côté, M. Masinia, D. Mourato. Comparison of membrane options for water reuse and reclamation Desalination, 167 (2004), pp. 1-11.

[4] R. Rosal, A. Rodríguez, J.A. Perdigón-Melón, A. Petre, E. García-Calvo, M.J. Gómez, A. Agüera, A.R. Fernández-Alba. Occurrence of emerging pollutants in urban wastewater and their removal through biological treatment followed by ozonation. Water Res., 44 (2010), pp. 578-588.

[5] M. Clara, B. Strenn, O. Gans, E. Martinez, N. Kreuzinger, H. Kroiss. Removal of selected pharmaceuticals, fragrances and endocrine disrupting compounds in a membrane bioreactor and conventional wastewater treatment plants. Water Res., 39 (2005), pp. 4797-4807.

[6] K. Katsoufidou, S.G. Yiantsios, A.J. Karabelas. A study of ultrafiltration membrane fouling by humic acids and flux recovery by backwashing: experiments and modeling. J. Membr. Sci., 266 (2005), pp. 40-50.

[7] Y. Ye, P. Le-Clech, V. Chen, T.A.G. Fane. Evolution of fouling during crossflow filtration of model EPS solutions. J. Membr. Sci., 264 (2005), pp. 190-199.

[8] P. Le-Clech, V. Chen, T.A.G. Fane. Fouling in membrane bioreactors used in wastewater treatment. J. Membr. Sci., 284 (2006), pp. 17-53.

[9] E. Agusa., N. Voutchkovb, D.L. Sedlak. Disinfection by-products and their potential impact on the quality of water produced by desalination systems: a literature review. Desalination, 237 (2009), pp. 214-237.

[10] H.C. Flemming, G. Schaule, T. Griebe, J. Schmitt, A. Tamachkiarowa. Biofouling—the Achilles heel of membrane processes. Desalination, 113 (1997), pp. 215-225.

[11] H.F. Ridgway, M.G. Rigby, D.G. Argo. Adhesion of a Mycobacterium sp. to cellulose diacetate membranes used in reverse osmosis. Appl. Environ. Microbiol., 47 (1984), pp. 61-67.

[12] C.X. Liu, D.R. Zhang, Y. He, X.S. Zhao, R. Bai. Modification of membrane surface for anti-biofouling performance: effect of anti-adhesion and anti-bacteria approaches. J. Membr. Sci., 346 (2010), pp. 121-130.

[13] H.Y. Yu, Z.K. Xu, Q. Yang, M.X. Hu, S.Y. Wang Improvement of the antifouling characteristics for polypropylene microporous membranes by the sequential photoinduced graft polymerization of acrylic acid. J. Membr. Sci., 281 (2006), pp. 658-665.

[14] R. Malaisamy, D. Berry, D. Holder, L. Raskin, L. Lepak, K.L. Jones. Development of reactive thin film polymer brush membranes to prevent biofouling. J. Membr. Sci., 350 (2010), pp. 361-370.

[15] Q.L. Feng, J. Wu, G.Q. Chen, F.Z. Cui, T.N. Kim, J.O. Kim. A mechanistic study of the antibacterial effect of silver ions on Escherichia coli and

Staphylococcus aureus. J. Biomed. Mater. Res. A, 52 (2000), pp. 662-668.
[16] A. Moriya, T. Maruyama, Y. Ohmukai, T. Sotani, H. Matsuyama. Preparation of poly(lactic acid) hollow fiber membranes via phase separation methods. J. Membr. Sci., 342 (1–2) (2009), pp. 307-312.
[17] F. Pignon, A. Magnin, J.M. Piau, G. Belina, P. Panine. Structure and orientation dynamics of sepiolite fibers–poly(ethylene oxide) aqueous suspensions under extensional and shear flow, probed by in situ SAXS. Rheol. Acta, 48 (2009), pp. 563-578.
[18] A. Esteban-Cubillo, R. Pina-Zapardiel, J.S. Moya, M.F. Barba, C. Pecharromán. The role of magnesium on the stability of crystalline sepiolite structure. J. Eur. Ceram. Soc., 28 (2008), pp. 1763-1768.
[19] C. Pecharroman, A. Esteban-Cubillo, I. Montero, J.S. Moya, E. Aguilar, J. Santaren, A. Álvarez. Monodisperse and corrosion-resistant metallic nanoparticles embedded into sepiolite particles for optical and magnetic applications. J. Am. Ceram. Soc., 89 (2006), pp. 3043-3049.
[20] C. Wilhelm, C. Billotey, J. Roger, J.N. Pons, J.C. Bacri, F. Gazeau. Intracellular uptake of anionic superparamagnetic nanoparticles as a function of their surface coating. Biomaterials, 24 (2003), pp. 1001-1011.
[21] Y.E. Lin, R.D. Vidic, J.E. Stout, V.L. Yu. Negative effect of high pH on biocidal efficacy of copper and silver ions in controlling *Legionella pneumophila*. Appl. Environ. Microbiol., 68 (2002), pp. 2711-2715.
[22] R.J. Griffitt, K. Hyndman, N.D. Denslow, D.S. Barber. Comparison of molecular and histological changes in zebrafish gills exposed to metallic nanoparticles. Toxicol. Sci., 107 (2009), pp. 404-415.
[23] L. Kiaune, N. Singhasemanon. In: D.M. Whitacre (Ed.), Pesticidal Copper (I) Oxide: Environmental Fate and Aquatic Toxicity Reviews of Environmental Contamination and Toxicology, vol. 213 (2011), pp. 1-26.
[24] K. Kasemets, A. Ivask, H.C. Dubourguier, A. Kahru. Toxicity of nanoparticles of ZnO, CuO and TiO_2 to yeast *Saccharomyces cerevisiae.* Toxicol. In Vitro, 23 (2009), pp. 1116-1122.
[25] E. Navarro, F. Piccapietra, B. Wagner, F. Marconi, R. Kaegi, N. Odzak, L. Sigg, R. Behra. Toxicity of Silver Nanoparticles to *Chlamydomonas reinhardtii*. Environ. Sci. Technol., 42 (2008), pp. 8959-8964.
[26] T.M. Benn, P. Westerhoff. Nanoparticle silver released into water from commercially available sock fabrics. Environ. Sci. Technol., 42 (2008), pp. 4133-4139.
[27] R. Kaegi, A. Voegelin, B. Sinnet, S. Zuleeg, H. Hagendorfer, M. Burkhardt, H. Siegrist. Behavior of metallic silver nanoparticles in a pilot wastewater treatment plant. Environ. Sci. Technol., 45 (2011), pp. 3902-3908.

https://doi.org/10.1016/j.memsci.2012.02.060